lithiated allylic alcohol in eq 2 was cyclized in 64% chemical yield;

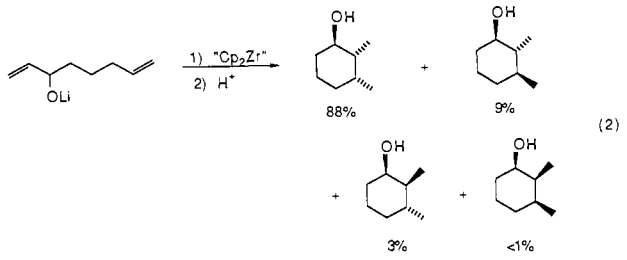

(2)

the 1,2-trans 1,3-cis isomer constituted 88% of the product. We intend to further explore and develop this potentially useful observation.

In summary, the zirconium-mediated cyclization of nonconjugated dienes provides an efficient, versatile,[13] and stereoselective route to functionalized carbocycles and heterocycles.

Supplementary Material Available: Details of the synthesis, isolation, and characterization (^{1}H NMR, ^{13}C NMR, HRMS, elemental analysis) for all reported products (8 pages). Ordering information is given on any current masthead page.

(13) Known limitations: Cyclization failed for 1,5-hexadiene and 1,8-nonadiene; diethyl diallylmalonate underwent competitive reduction of the carbonyl group; substrates containing the allyl ether functionality gave significantly diminished yields.

An ENDOR Study of Spin Distributions in Octaethylmetalloporphyrin π Cation Radicals

P. O. Sandusky, A. Salehi,† C. K. Chang,* and G. T. Babcock*

Department of Chemistry
Michigan State University
East Lansing, Michigan 48824

Received March 7, 1989

π cation radicals of the metalloporphyrin family are biologically important species, found as primary products of the photochemical reaction in photosynthetic reaction centers and as oxidized intermediates in the enzymatic cycles of horseradish peroxidase and catalase.[1] Classic ESR studies by Fajer and co-workers have demonstrated that stable porphyrin π cation radicals of either the $^2A_{2u}$ or $^2A_{1u}$ ground state can be formed. $^2A_{2u}$ species such as Zn tetraphenylporphyrin radical are distinguishable by large, ESR resolvable nitrogen hyperfine couplings, whereas the ESR spectra of $^2A_{1u}$ complexes, such as Mg octaethylporphyrin radical ($MgOEP^+$), display either meso proton couplings of only moderate size or no resolved structure at all.[2] For systems without evident hyperfine structure attempts have been made to assign ground states based on optical spectra; the visible spectra of $Co^{III}OEP^{\cdot+}2Br^-$ and $Co^{III}OEP^{\cdot+}2Cl^-$ are thought to be characteristic of $^2A_{1u}$ radicals, whereas the distinctive spectra of $Cu^{II}OEP^{\cdot+}2ClO_4^-$ and $Co^{III}OEP^{\cdot+}2ClO_4^-$ were taken as signatures of the $^2A_{2u}$ state.[3] Although these assignments have formed the basis for much of the discussion in the porphyrin radical literature,[4] they have been brought into question by several independent EPR,[5] NMR,[6] and resonance Raman studies.[7] ESR hyperfine coupling is the physical parameter most unequivocally related to electron spin density in organic radicals; unfortunately, none of the ESR spectra of the principal species in question ($Cu^{II}OEP^{\cdot+}2ClO_4^-$, $Co^{III}OEP^{\cdot+}2ClO_4^-$, $Co^{III}OEP^{\cdot+}2Br^-$, $Co^{III}OEP^{\cdot+}2Cl^-$) display resolved hyperfine structure.[8] We report here measurements of

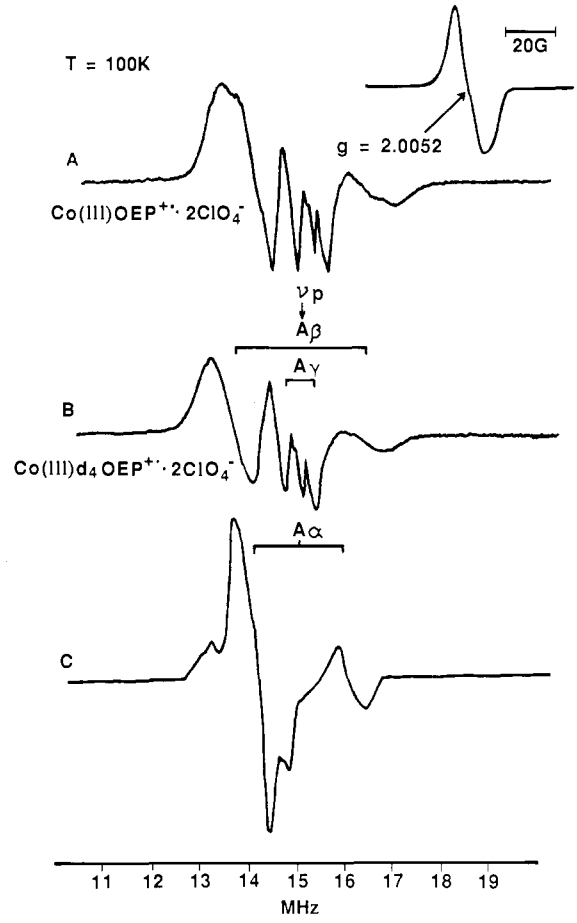

Figure 1. ESR and proton ENDOR spectra of $Co^{III}OEP^{\cdot+}2ClO_4^-$ glassed in 1:1 CH_2Cl_2/toluene at 100 K. Insert: ESR spectrum, 0.65 mW microwave power, 0.5 G_{pp} 12.5 KHz field modulation, 200 s sweep time, 200 ms time constant. A: ENDOR spectrum of 1 mM $Co^{III}OEP^{\cdot+}2ClO_4^-$. B: ENDOR spectrum of 1 mM $Co^{III}d_4OEP^{\cdot+}2ClO_4^-$. ENDOR spectra were taken at 16 mW micowave power, 150 W rf power, 25 KHz rf modulation, 2000 s sweep time, 2 s time constant, with the magnetic field set at 3458.0 G (9.7027 GHz). C: Difference of spectra A and B showing meso proton ENDOR features (note that the ordinate scale has been expanded).

† Present address: Department of Chemistry, University of California-Santa Barbara, Santa Barbara, CA 93106.

(1) (a) Dolphin, D.; Felton, R. H. *Acc. Chem. Res.* **1974**, *7*, 26-32. (b) Frew, J. E.; Jones, P. In *Advances in Inorganic and Bioinorganic Mechanism*; Academic Press; New York, 1984; Vol. 3, pp 175-215.

(2) (a) Fajer, J.; Davis, M. S. In *The Porphyrins*; Dolphin, D., Ed.; Academic Press: New York, 1979; Vol. 4, pp 197-256. (b) Fajer, J.; Borg, D. C.; Forman, A.; Felton, R. H.; Vegh, L.; Dolphin, D. *Ann. N.Y. Acad. Sci.* **1973**, *206*, 349-364.

(3) Dolphin, D.; Forman, A.; Borg, D. C.; Fajer, J.; Felton, R. H. *Proc. Natl. Acad. Sci. U.S.A.* **1971**, *68*, 614-618.

(4) (a) Edwards, W. D.; Zerner, M. C. *Can. J. Chem.* **1986**, *63*, 1763-1772. (b) DiNello, R. K.; Dolphin, D. H. *J. Biol. Chem.* **1981**, *256*, 6903-6912. (c) Hanson, L. K.; Chang, C. K.; Davis, M. S.; Fajer, J. *J. Am. Chem. Soc.* **1981**, *103*, 663-670. (d) Browett, W. R.; Stillman, M. J. *Biochim. Biophys. Acta* **1981**, *660*, 1-7. (e) Gasyna, Z.; Browett, W. R.; Stillman, M. J. *Inorg. Chem.* **1988**, *27*, 4619-4622. (f) Kim, D.; Miller, L. A.; Rakhit, G.; Spiro, T. G. *J. Phys. Chem.* **1986**, *90*, 3320-3325.

(5) Rutter, R.; Valentine, M.; Hendrich, M. P.; Hager, L. P.; Debrunner, P. G. *Biochemistry* **1986**, *22*, 4769-4774.

(6) (a) Morishma, I.; Takamuki, Y.; Shiro, Y. *J. Am. Chem. Soc.* **1984**, *106*, 7666-7672. (b) Godziela, G. M.; Goff, H. M. *J. Am. Chem. Soc.* **1986**, *108*, 2237-2243.

(7) (a) Oertling, W. A.; Salehi, A.; Chang, C. K.; Babcock, G. T. *J. Phys. Chem.* **1989**, *93*, 1311-1319. (b) Oertling, W. A.; Salehi, A.; Chung, Y. C.; Leroi, G. E.; Chang, C. K.; Babcock, G. T. *J. Phys. Chem.* **1987**, *91*, 5887-5898. (c) Czernuszewicz, R. S.; Macor, K. A.; Li, X. Y.; Kincaid, J. R.; Spiro, T. G. *J. Am. Chem. Soc.*, submitted for publication.

0002-7863/89/1511-6437$01.50/0

Table I. ^{1}H Hyperfine Constants (MHz) for MOEP$^+$ Radicals

	$Co^{III}OEP^+$				
	ClO_4^-	Cl^-	$MgOEP^+$	$^2A_{2u}$[a]	$^2A_{1u}$[a]
meso-α	1.9	4.0–5.0	4.1[b]	14.7	0.1
ethyl-β	2.6	2.1	2.0	1.2	2.4
ethyl-γ	0.6	0.5	0.5		

[a] Based on Q values from ref 2a and calculated spin densities from ref 4a and 15. [b] Resolved in ESR spectrum (ref 2a).

^{1}H hyperfine couplings for $Co^{III}OEP^{\bullet+}2ClO_4^-$ and $Co^{III}OEP^{\bullet+}$-$2Cl^-$, which were resolved by using ENDOR spectroscopy. Based on the magnitudes of the meso proton hyperfine constants, we conclude that the ground states of both species are predominately $^2A_{1u}$.

Because the ESR spectra of the chloride and bromide ligated species of $Co^{III}OEP^+$ proved difficult to power saturate in fluid methylene chloride solutions, our ENDOR spectroscopy was done on optical quality 1:1 methylene chloride/toluene glasses at 100 K.[9-11] Spectrometer settings were chosen so as to optimize the resolution of the various ENDOR signals we observed. Owing to different microwave power saturation characteristics, the optimal instrument settings for the halide ligated and perchlorate ligated species were different. Optical spectra of the glassed ENDOR samples, taken at 100 K on a Perkin Elmer Lambda 5 spectrophotometer equipped with a N_2 flow dewar, were identical with the spectra of the fluid solutions taken at 298 K and essentially identical with previously published room-temperature spectra of $Co^{III}OEP^{\bullet+}2ClO_4^-$, $Co^{III}OEP^{\bullet+}2Br^-$, and $Co^{III}OEP^{\bullet+}2Cl^-$.[3,7b,8] The chloride and bromide ligated species have nearly identical visible spectra.

The ENDOR spectrum of $Co^{III}d_4OEP^{\bullet+}2ClO_4^-$ readily allows the assignment of the ethyl β and ethyl γ hyperfine couplings as 2.6 and 0.6 MHz, respectively (Figure 1B).[12] Although the $Co^{III}OEP^{\bullet+}2ClO_4^-$ meso α proton and ethyl β proton bands overlap (Figure 1 (parts A and B)), a fairly clear picture of the α proton hyperfine powder pattern is resolved by subtracting the spectrum of the meso-deuterated complex (Figure 1C). The meso proton features display a rhombic powder pattern with turning points at 3.1, 1.8, and 0.8 MHz (A_{iso} = 1.9 MHz).[13,14] The ethyl β and ethyl γ couplings observed in the $Co^{III}OEP^{\bullet+}2Cl^-$ ENDOR spectra are comparable to those found in the perchlorate ligated species (Figure 2, Table I). In the spectrum of the chloride ligated complex the ethyl bands obscure one of the three sets of the meso proton turning point features. However, from the two resolved powder pattern features the α proton A_{iso} can be estimated as being between 4 and 5 MHz.

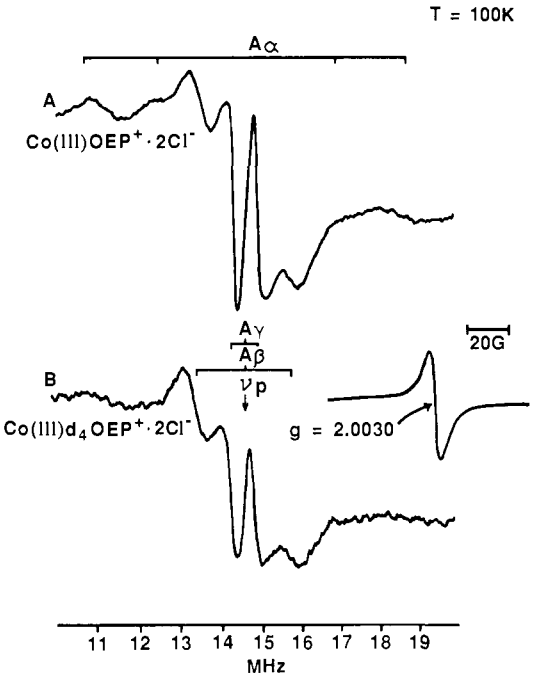

Figure 2. ESR and ENDOR spectra of $Co^{III}OEP^{\bullet+}2Cl^-$ glassed in 1:1 CD_2Cl_2-d_8-toluene at 100 K. Insert: ESR spectrum taken at 0.65 mW microwave power, 0.5 G_{pp} 12.5 KHz field modulation, 200 s sweep time, 200 ms time constant. A: ENDOR spectrum of 1 mM $Co^{III}OEP^{\bullet+}2Cl^-$. B: ENDOR spectrum of 1 mM $Co^{III}d_4OEP^{\bullet+}2Cl^-$. ENDOR spectra were taken at 32.4 mW microwave power, 150 W rf power, 150 KHz rf modulation, 2000 s sweep time, 10 s time constant, with the magnetic field set at 3461.0 G (9.7033 GHz).

From the McConnell relation ($A_{iso} = Q\rho$; Q = −76 MHz) and spin densities derived from SCF MO calculations,[2a,4a,15] the meso proton isotropic hyperfine couplings are predicted to be large in $^2A_{2u}$ ground-state radicals but very small in $^2A_{1u}$ systems (Table I). The meso proton hyperfine coupling constant in the chloride ligated $Co^{III}OEP^+$ species is comparable to that observed for the prototypical $^2A_{1u}$ radical, $MgOEP^+$,[2a] and it is noteworthy that the visible spectra of these two species are quite similar. The meso coupling of the perchlorate adduct is even smaller than that of $Co^{III}OEP^{\bullet+}2Cl^-$, and we thus conclude that the ground states of both species are predominantly $^2A_{1u}$ in character. The perchlorate ligated species is, if anything, less "$^2A_{2u}$-like" than the chloride ligated form. Our results are in qualitative agreement with NMR meso protons shifts indicating greater spin density at the meso carbon in $Co^{III}OEP^{\bullet+}2Br^-$ relative to $Co^{III}OEP^{\bullet+}2ClO_4^-$; however, we are puzzled by the lack of temperature dependence reported for the NMR shifts.[6b]

The meso proton couplings of $MgOEP^+$, $Co^{III}OEP^{\bullet+}2Cl^-$, and $Co^{III}OEP^{\bullet+}2ClO_4^-$ are all similar and close to those predicted for $^2A_{1u}$ orbital occupancy. They are, however, somewhat larger than would be expected for a purely $^2A_{1u}$ ground state (Table I). Similarly, we have observed a ~1.5 G ^{15}N coupling in the ENDOR spectrum of $Co^{III}OEP^{\bullet+}2ClO_4^-$. This splitting is significantly

(8) The ESR spectrum of $Cu^{II}OEP^{\bullet+}2ClO_4^-$ is complicated by coupling of the Cu(II) S = 1/2 and π cation radical (ref 6b). $Co^{III}OEP^{\bullet+}2ClO_4^-$, which is equivalent to the Cu(II) species in terms of its optical spectrum, has a narrow structureless ESR spectrum (7.5 G_{pp}), while the ESR spectrum of $Co^{III}OEP^{\bullet+}2Br^-$ is lifetime broadened by relaxation coupling to the ligating bromides (50 G_{pp} at −50 °C, ref 3). $Co^{III}OEP^{\bullet+}2Cl^-$ has been identified by its optical spectrum, which resembles that of the bromide ligated species, but has never previously been characterized by ESR in the literature (Setsune, J.; Ikeda, M.; Kishimoto, Y.; Kitao, T. *J. Am. Chem. Soc.* **1986**, *108*, 1309–1311).

(9) $Co^{II}OEP$ and $Co^{II}d_4OEP$ were synthesized as previously described. (a) Wang, C. B.; Chang, C. K. *Synthesis* **1979**, 548–549. (b) Fuhrhop, J. H.; Smith, K. M. In *Porphyrins and Metalloporphyrins*; Smith, K. M., Ed.; Elsevier: Amsterdam, 1975; pp 765–766, 816–817. (c) Falk, J. E. In *Porphyrins and Metalloporphyrins*; Elsevier: New York, 1964; p 798.

(10) The perchlorate, bromide, and chloride ligated $Co^{III}OEP^+$ species were prepared by using $Fe^{III}(ClO_4^-)_3$(s), Br_2(l), and Cl_2(g), respectively, as oxidants (ref 3, 7a, and 8).

(11) For description of ESR and ENDOR instrumentation, see: (a) O'Malley, P. J.; Babcock, G. T. *J. Am. Chem. Soc.* **1986**, *108*, 3995–4001. (b) Bender, C. J.; Sahlin, M.; Babcock, G. T.; Barry, B. A.; Chandrashekar, T. K.; Salowe, S. P.; Stubbe, J.; Lindstrom, B.; Petersson, L.; Ehrenberg, A.; Sjoberg, B.-M. *J. Am. Chem. Soc.*, submitted for publication.

(12) The relative magnitudes of the OEP ethyl γ and ethyl β hyperfine couplings, which have been determined for $Cu^{II}OEP^+$ and $Au^{II}OEP^+$ by NMR shifts, are similar to those we observe for $Co^{III}OEP^{\bullet+}2Cl^-$ and $Co^{III}OEP^{\bullet+}$-$2ClO_4^-$ (ref 6b). In all cases the γ proton coupling constant is 16–25% of the β proton coupling.

(13) For an organic radical in a disordered matrix, α proton ENDOR lines often display a rhombic powder pattern with turning points at $1.5A_{iso}$, A_{iso}, and $0.5A_{iso}$. (a) McConnell, H. M.; Heller, C.; Cole, T.; Fessenden, R. W. *J. Am. Chem. Soc.* **1960**, *82*, 766. (b) Pooley, D.; Whiffen, D. H. *Mol. Phys.* **1961**, *4*, 81. However, deviation from this pattern may occur if there are relatively large spin densities on adjacent ring carbons (ref 11a). (c) Hirota, N.; Hutchison, C. A., Jr.; Palmer, P. *J. Chem. Phys.* **1964**, *40*, 3717. (d) Bohme, U. R.; Wolf, H. C. *Chem. Phys. Lett.* **1972**, *17*, 582. In either case the A_{iso} can be calculated by taking the average of the powder pattern turning points.

(14) All of the ENDOR features of the perchlorate ligated $Co^{III}OEP^+$ species, whether meso α proton, ethyl β proton, or ethyl γ proton in origin, are more intense in the lower half of the spectrum. This may indicate that a cross relaxation step ($\Delta m_s + \Delta m_I = 0$) is involved in the radio frequency enhanced relaxation pathways. Kevan, L.; Kispert, L. D. *Electron Spin Double Resonance Spectroscopy*; John Wiley and Sons: New York, 1976.

(15) Fajer, J.; Borg, D. C.; Forman, A.; Dolphin, D.; Felton, R. H. *J. Am. Chem. Soc.* **1970**, *92*, 3451–3459.

smaller than the 2.2–2.9 G ^{15}N couplings observed in $^2A_{2u}$ systems such as ZnTPP$^+$.[2] The nitrogen hyperfine coupling in a $^2A_{1u}$ radical has never been measured directly; however, an estimate of 1 G for a ^{15}N coupling would seem reasonable for a purely $^2A_{1u}$ ground state.[2,15,16] Thus the couplings we observe suggest that some mixing of the $^2A_{2u}$ state into the $^2A_{1u}$ ground state may occur. This type of mixing has earlier been proposed by O'Malley and Babcock to account for ^1H couplings observed in the ENDOR spectrum of the oxidized reaction center chlorophyll in the Photosystem I of plant photosynthetic membranes.[17] Recently, Czernuszewicz et al. have addressed this question for MgOEP$^+$ and have concluded from Raman spectra that the A_{2g} vibrational modes mix the $^2A_{2u}$ state into a predominately $^2A_{1u}$ ground state.[7c] While the possibility of orbital mixing and the mechanism by which it may occur remain to be settled, the ENDOR data we have presented here indicate that both the dihalide and diperchlorate cations are predominately $^2A_{1u}$ in character, regardless of their visible absorption spectra.

Acknowledgment. P.O.S. thanks W. A. Oertling for many helpful discussions. This research was supported by NIH Grants GM37300 (G.T.B.) and GM36520 (C.K.C.).

(16) Vincow, G. In *Radical Ions*; Kaiser, E. T., Kevan, L., Eds.; Interscience: New York, 1968; pp 151–209.
(17) O'Malley, P. J.; Babcock, G. T. *Proc. Natl. Acad. Sci. U.S.A.* **1984**, 1098–1101.

Time-Resolved Raman Detection of ν(Fe–O) in an Early Intermediate in the Reduction of O_2 by Cytochrome Oxidase

Constantinos Varotsis,[†] William H. Woodruff,[‡] and Gerald T. Babcock*,[†]

Department of Chemistry, Michigan State University
East Lansing, Michigan 48824
INC/4 Mail Stop C-346
Los Alamos National Laboratory
Los Alamos, New Mexico 87545

Received March 23, 1989

Cytochrome oxidase contains four redox-active centers per functional unit: cytochromes *a* and a_3 and the copper atoms, Cu_A and Cu_B. Cytochrome *c*, the physiological substrate of cytochrome oxidase, transfers electrons to the cyt *a* and Cu_A sites. These reducing equivalents are transferred to the binuclear cyt a_3···Cu_B center, which binds O_2 and reduces it to H_2O. Although the reaction between O_2 and cytochrome oxidase occurs too quickly to be studied by conventional stopped-flow techniques, Gibson and Greenwood[1] showed that photolysis of the cytochrome a_3^{2+}–CO complex of the enzyme in the presence of O_2 could be used to circumvent this limitation. Babcock et al.[2] adopted this approach and used time-resolved resonance Raman spectroscopy to study the reaction of fully and partially reduced cytochrome oxidase with O_2. Although instrumental limitations restricted data acquisition to the high-frequency (>1000 cm^{-1}) range, they concluded that the reoxidation of cytochrome oxidase proceeds via a cytochrome a_3^{2+}–O_2 complex that resembles oxymyoglobin and oxyhemoglobin. Direct detection of iron/bound oxygen ligand vibrations is necessary to test these conclusions as well as to provide detailed information on subsequent intermediates in the dioxygen reduction reaction. To this end we have developed techniques that allow us to carry out low-frequency Raman detection under flow/flash conditions; here we report $\nu(Fe^{2+}–O)$ for an early intermediate in the cytochrome oxidase/dioxygen reaction. Consideration of data on dioxygen adducts of other heme proteins and model hemes indicates that this early intermediate is most likely the cytochrome a_3^{2+}–O_2 complex. Its $\nu(Fe^{2+}–O_2)$ frequency is elevated relative to that observed for the other systems, however, from which we conclude that already at 10 μs in the oxidase reaction the O=O bond is weakened, presumably in preparation for its rupture in subsequent steps in the reaction.

The experimental techniques used for the measurements of time-resolved Raman spectra have already been reported[2b] with the exceptions that the scattering volume was a free jet in air and that 427-nm excitation was used as the probe wavelength.[3] The

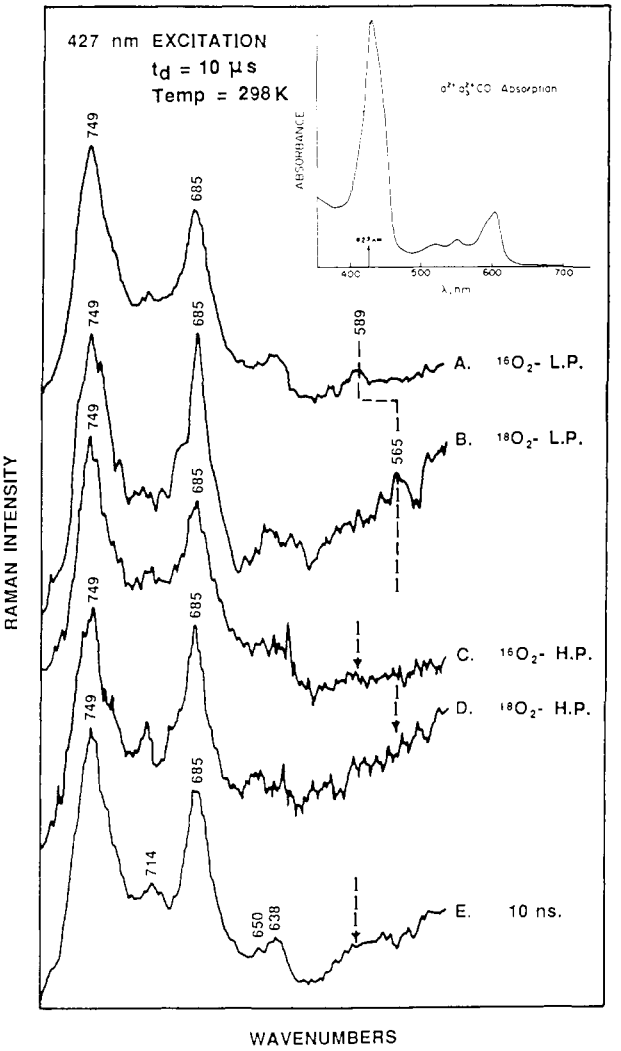

Figure 1. Time-resolved resonance Raman spectra of cytochrome oxidase following initiation of the reaction with oxygen at room temperature. The energy of the 532-nm photolysis pump pulse was 1.3 mJ, sufficient to photolyze the enzyme–CO complex and initiate the O_2 reduction reaction. The energy of the probe beam was 0.3 mJ for spectra A and B[14] and 1.0 mJ for spectra C–E. The repetition rate for both the pump and probe pulses (10-ns duration) was 10 Hz. The pump–probe delay was 10 μs for spectra A–D and 10 ns for transient spectrum E. The accumulation time was 110 min for spectrum A, 70 min for spectrum B, 5 min for spectra C and D, and 15 min for spectrum E.

[†] Michigan State University.
[‡] Los Alamos National Laboratory.

(1) (a) Gibson, Q.; Greenwood, C. *Biochem. J.* **1963**, *86*, 541. (b) Greenwood, C.; Gibson, Q. *J. Biol. Chem.* **1967**, *242*, 1782. (c) Greenwood, C.; Hill, B. *Biochem. J.* **1984**, *218*, 913. (d) Hill, B.; Greenwood, C.; Nichols, P. *Biochim. Biophys. Acta* **1986**, *853*, 91. (e) This technique has been modified for low-temperature application by Chance and co-workers and has been used to study the oxidase/O_2 reaction in frozen samples by several groups. See: Chance, B.; Saronio, C.; Leigh, J. S. *J. Biol. Chem.* **1975**, *250*, 9226. Clore, G. M.; Andreasson, L. E.; Karlsson, B.; Aasa, R.; Malmstrom, B. G. *Biochem. J.* **1980**, *185*, 139. Chan, S. I.; Witt, S. N.; Blair, D. F. *Chem. Scr.* **1988**, *28A*, 51. For a review, see: Naqui, A.; Chance, B. *Annu. Rev. Biochem.* **1986**, *55*, 137.

(2) (a) Babcock, G. T.; Jean, J. M.; Johnston, L. N.; Palmer, G.; Woodruff, W. H. *J. Am. Chem. Soc.* **1984**, *106*, 8305. (b) Babcock, G. T.; Jean, J. M.; Johnston, L. N.; Woodruff, W. H.; Palmer, G. *J. Inorg. Biochem.* **1985**, *23*, 243. (c) Babcock, G. T. *Biological Applications of Raman Scattering*; Spiro, T. G., Ed.; Academic Press: New York, 1988; Vol. 3, p 295.

0002-7863/89/1511-6439$01.50/0